韓國水資源學會論文集
第38卷 第1號 · 2005年 1月
pp. 83~96

해안방조제가 조류 및 잔류흐름에 미치는 영향

The Effects of Tidal Currents and Residual Flow on the Sea Dike

백 중 철* / 윤 영 호** / 신 문 섭*** / Dinh Van Manh****
Park, Joongcheol / Yoon,Young-Ho / Shin, Moon-Seup / Manh, Dinh Van

Abstract

Three-dimensional hydrodynamic numerical simulation is carried out to investigate the effects of the coastal land reclamation on the marine hydrodynamics, environment and ecosystem. The changes of tide, tidal currents and residual currents, including tide-induced, wind driven and density driven components due to the construction of the sea dike system are simulated numerically. The governing equations transformed into σ-coordinates are solved by an implicit finite difference method. The numerical model is calibrated using the tide charts of 4 major tidal constituents, M_2, S_2, K_1 and O_1. The numerical solutions show that there are significant changes of residual currents, especially induced by both tidal and wind-driven currents.

Keywords : sea dike, three-dimensional hydrodynamic numerical model, tidal current, residual current.

요 지

해안매립이 해양의 동수력학, 환경 및 생태계에 미치는 영향을 분석하기 위하여 3차원 동수력학 수치해석을 실시하였다. 이 연구에서는 방조제 건설에 따른 조석, 바람 및 밀도변화 성분을 포함한 조류와 잔차류의 변화를 수치모의하였다. σ-좌표로 변환된 지배방정식은 음해유한차분법을 이용하여 해석하였다. 수치모형은 조석의 4대 주요 구성성분인 M_2, S_2, K_1 및 O_1의 조석표를 이용하여 검증하였다. 수치해석결과, 주로 조석 및 바람에 의한 잔차류의 변화가 큰 것으로 나타났다.

핵심용어 : 방조제, 3차원 동수력학 수치모형, 조류, 잔차류

1. Introduction

The land reclamation area of Saemangeum (Kunsan) is located between 126°10′E - 126°50′E and 35°35′N - 36°05′N at the western coast of the Korean peninsula. This area consists of lots of small islands including wide areas of semi-diurnally flooded and dewatered tidal flats. The reclamation area of Saemangeum has a range of 5.6m spring tide and the maximum tidal current speed reaches

* 조지아공대 토목환경공학과 연구원
Research Engineer, School of Civil and Environmental Engineering, Georgia Institute of Technology, Atlant, GA, 30335-0355.
(e-mail: joongcheol.paik@ce.gatech.edu)
** 강원도립대학 건설시스템과 조교수
Assistant Professor, Departmentof Civil Engineering, Gangwon Provincial University, Gangneung, Gangwon, 210-804.
(e-mail: yhyoon@gw.ac.kr)
*** 군산대학교 토목환경공학부 교수
Professor, School of Civil Engineering, Kunsan National University, 68 Miryong-dong, Kunsan, Chonbuk, Korea.
(e-mail: seup@kunsan.ac.kr)
**** Senior researcher, Institute of Mechanics, NCST, 264 Doican, Hanoi, Vietnam.
(e-mail: hoanghai_01@yahoo.com)

around 1.41 m/sec in ordinary spring tide. Most of the sediments deposited on the tidal flats are transported from the Geum river, the Mankyung river and the Dongjin river. The soil in this area consists of silty sand with the depth of 10m to 30m. The wind in winter is strong from the direction of northwest. In the past twenty years, land reclamation projects for agricultural purpose or industrial complex have been mostly implemented along the western coast of Korea.

The 33km sea dike and 40,100ha reclamation area is being constructed in the Saemangeum area. These large-scale coastal land reclamation works can give important effects on the change of the hydro-dynamics, the marine environment and ecosystem in this area (Choi, 1990; Shin, et al., 1994; Kim, et al., 1997; Park, 2000; Lee, et al., 2003). These negative effects on the marine aquaculture and ecosystem are mainly induced by common coastal construction practices directly or potentially. The purpose of mitigation is threefold: 1) to harmonize the development and the conservation of environment, 2) to restrict environmental destruction, and 3) to recover the environment damaged by the construction in the coastal region.

In this paper, we have applied a three-dimensional hydrodynamic numerical model to investigate the changes of marine hydrodynamics, namely the tide, tidal currents and residual currents including tide-induced residual, wind driven and density driven components in the reclamation area. We develop an implicit finite difference numerical model for the reclamation area under the condition before and after the dike system construction and simulate the propagation of 4 major tidal constituents, M_2, S_2, O_1 and K_1. The numerical model was calibrated using the observed data on tide and tidal currents of M_2 which is the most important constituent in this area. Based on the tidal calculations and data on wind, sea water temperature and salinity, the effects of the sea dike construction on residual flows in both summer and winter were investigated.

2. Governing Equations

On the valid assumption that the shallow water is measured when the vertical length scale is much smaller than the horizontal one, the flow is governed the momentum equations, continuity equation and the transport equations for the scalar such as the temperature and the salinity. By invoking the Boussinesq hypothesis to express the Reynolds stresses in terms of the mean rate of strain tensor, these governing equations can be expressed as follows:

Momentum equations

$$\frac{\partial u}{\partial t}+u\frac{\partial u}{\partial x}+v\frac{\partial u}{\partial y}+w\frac{\partial u}{\partial z}-fv=-\frac{1}{\rho}\frac{\partial p}{\partial x}+\frac{\partial}{\partial x}(A_h\frac{\partial u}{\partial x})+\frac{\partial}{\partial y}(A_h\frac{\partial u}{\partial y})+\frac{\partial}{\partial z}(A_v\frac{\partial u}{\partial z})+F_x \tag{1}$$

$$\frac{\partial v}{\partial t}+u\frac{\partial v}{\partial x}+v\frac{\partial v}{\partial y}+w\frac{\partial v}{\partial z}+fu=-\frac{1}{\rho}\frac{\partial p}{\partial y}+\frac{\partial}{\partial x}(A_h\frac{\partial v}{\partial x})+\frac{\partial}{\partial y}(A_h\frac{\partial v}{\partial y})+\frac{\partial}{\partial z}(A_v\frac{\partial v}{\partial z})+F_y \tag{2}$$

where

$$p=\rho_o g\zeta+\int_z^\zeta g\frac{\rho-\rho_o}{\rho_o}dz,\quad \rho=\rho(T,S,p) \tag{3}$$

$$F_x=\frac{\partial}{\partial x}(A_h\frac{\partial u}{\partial x})+\frac{\partial}{\partial y}(A_h\frac{\partial u}{\partial y})+\frac{1}{\rho}\frac{\partial S_{xx}}{\partial y}+\frac{1}{\rho}\frac{\partial S_{xy}}{\partial x} \tag{4}$$

$$F_y=\frac{\partial}{\partial x}(A_h\frac{\partial v}{\partial x})+\frac{\partial}{\partial y}(A_h\frac{\partial v}{\partial y})+\frac{1}{\rho}\frac{\partial S_{yy}}{\partial y}+\frac{1}{\rho}\frac{\partial S_{yx}}{\partial x} \tag{5}$$

Continuity equation

$$\frac{\partial u}{\partial x}+\frac{\partial v}{\partial y}+\frac{\partial w}{\partial z}=0 \tag{6}$$

Temperature transport equation

$$\frac{\partial T}{\partial t}+u\frac{\partial T}{\partial x}+v\frac{\partial T}{\partial y}+w\frac{\partial T}{\partial z}=\frac{\partial}{\partial x}(D_h\frac{\partial T}{\partial x})+\frac{\partial}{\partial y}(D_h\frac{\partial T}{\partial y})+\frac{\partial}{\partial z}(D_v\frac{\partial T}{\partial z}) \tag{7}$$

Salinity transport equation

$$\frac{\partial S}{\partial t}+u\frac{\partial S}{\partial x}+v\frac{\partial S}{\partial y}+w\frac{\partial S}{\partial z}=\frac{\partial}{\partial x}(D_h\frac{\partial S}{\partial x})+\frac{\partial}{\partial y}(D_h\frac{\partial S}{\partial y})+\frac{\partial}{\partial z}(D_v\frac{\partial S}{\partial z}) \tag{8}$$

where u, v, w are velocity components in x, y, z directions, respectively; f is the Coriolis parameter (=2 $\omega\sin\varphi$, ω is the angular velocity of the earth's rotation, φ is latitude); g (=980 cm/s^2) is the acceleration due to gravity; t is the time; p is the water pressure; ρ is the water density, ρ_o is the overall mean water density; is the sea level height

above the mean sea surface; T and S are the sea water temperature and salinity; A_h and D_h are the horizontal eddy viscosity and diffusivity; and A_v and D_v are the vertical eddy viscosity and diffusivity, respectively. S_{xx} is x component tidal stress in x direction, S_{xy} is y component tidal stress in x direction, S_{yx} is x component tidal stress in y direction, S_{yy} is y component tidal stress in y direction The vertical velocity component w, computed from the solution of the continuity equation (6), can be neglected in the equations of motion (1) and (2).

Turbulence closure

The above governing equations contain parameterized Reynolds stress terms that account for the turbulent diffusion of momentum. The vertical eddy viscosity A_v in equations (1) and (2) can be calculated by applying a second order turbulence closure method in which the Reynolds stresses are characterized by the equations for the turbulence kinetic energy, $q^2/2$ and a turbulence macro scale l (Mellor and Yamada, 1982).

$$\frac{\partial q^2}{\partial t}+\rho\nabla q^2=\frac{\partial}{\partial z}(K_q\frac{\partial q^2}{\partial z})+2A_v\left[(\frac{\partial u}{\partial z})^2+(\frac{\partial v}{\partial z})^2\right]+\frac{2gK_H}{\rho_0}\frac{\partial\rho}{\partial z}-\frac{2q^3}{B_1 l}+F_q \tag{9}$$

$$\frac{\partial q^2 l}{\partial t}+\rho\nabla q^2 l=\frac{\partial}{\partial z}(K_q\frac{\partial q^2 l}{\partial z})+lE_1A_v\left[(\frac{\partial u}{\partial z})^2+(\frac{\partial v}{\partial z})^2\right]+\frac{lE_1gK_H}{\rho_0}\frac{\partial\rho}{\partial z}-\frac{q^3}{B_1}\tilde{W}+F_l \tag{10}$$

where

$$\tilde{W}\equiv 1+E_2(\frac{l}{\kappa L})^2,\quad \frac{1}{L}\equiv\frac{1}{\zeta-z}+\frac{1}{H+z} \tag{11}$$

Where κ (=0.4) is the von Karman constant; the term F_q and F_l are horizontal mixing.

3. Numerical Method

The governing equations are transformed into the σ coordinates and then solved by a finite difference method. Due to space considerations, a brief description of the numerical methods is given in this paper (see Manh and Yanagi, 1997 for details). The numerical method can be summarized as three steps: 1) the modified shallow water equations obtained by integrating the continuity and momentum equations over the depth are solved by an alternative direction implicit (ADI) scheme; 2) The momentum and scalar transport equations are solved by the ADI scheme in the vertical direction to determine the distributions of horizontal velocity; and 3) the vertical velocity is calculated by integrating the continuity equation over the depth and the sea water density determined by the state equation. The boundaries such as the sea surface, bottom, lateral solid wall and free stream utilize fairly simple and robust boundary conditions as:

At the sea surface

$$\frac{\partial\zeta}{\partial t}+u\frac{\partial\zeta}{\partial x}+v\frac{\partial\zeta}{\partial y}-w=0, \tag{12}$$

$$\rho A_v\frac{\partial u}{\partial z}=\tau_x^s,\quad \rho A_v\frac{\partial v}{\partial z}=\tau_y^s,\quad (\tau_x^s,\tau_y^s)=\rho_a C_d\sqrt{W_x^2+W_x^2}(W_x,W_y) \tag{13}$$

$$q^2=B_1^{2/3}V_S^2,\quad q^2 l=0 \tag{14}$$

At the bottom

$$u\frac{\partial h}{\partial x}+v\frac{\partial h}{\partial y}+w=0, \tag{15}$$

$$\rho A_v\frac{\partial u}{\partial z}=\tau_x^b,\quad \rho A_v\frac{\partial v}{\partial z}=\tau_y^b,\quad (\tau_x^b,\tau_y^b)=\beta\sqrt{(u_*^2+v_*^2)}(u_*,v_*) \tag{16}$$

$$q^2=B_1^{2/3}V_B^2,\quad q^2 l=0 \tag{17}$$

At the lateral solid boundary

$$v_n=0 \tag{18}$$

At the open boundary

One of the following hydrodynamic conditions is used:

(1) given sea water levels;
(2) prefixed volume transports; or
(3) radiation condition.

Here ρ_a is the air density, C_d is the sea surface drag coefficient, W_x and W_y are the components of the wind vector, V_B and V_S are the friction velocity at the surface and bottom, respectively, β is the bottom friction coefficient, the subscript $(*)$ indicates the value near the bottom, and n the unit outward vector. τ_x^s and τ_y^s are x and y component of sea-surface drag, τ_x^b and τ_y^b are x and y component of sea-bottom drag, h is the water depth.

4. Setup and Calibration of the Numerical Model

The numerical model is set up for the Saemangeum area with the extent of about 45 km wide and 54 km long, as shown in Fig. 1. The depth data are taken based on the map on a scale of 1:75,000. The horizontal grid sizes are 200m and water column is divided into 10 equal layers in the numerical model. The west, north and south sides of the study area are all open boundary.

In order to simulate the propagations of 4 major tidal constituents, the sea water levels are specified along the open boundaries on the basic of their harmonic constants, respectively. The radiation condition is applied in the cases of residual flow calculations. The computational scenarios are divided into three groups, before (called Case B), after the sea dike construction with three flow gates (Case A) and without flow gates (Case A-2). That means the existence of the sea dike system is taken into account in the second and third computational scenarios groups, Case A and Case A-2.

The observational data on tide and tidal currents are obtained from the field survey carried out by the Rural Development Corporation in Korea. The locations of measurement, 94-R-3 and 94-R-4, are shown in Fig. 1. The tidal harmonic constants of M_2, S_2, K_1 and O_1 are got from tide charts of National Oceanographic Research Institute and at 2 tide gauge stations Kunsan outer Harbour and Wi Island.

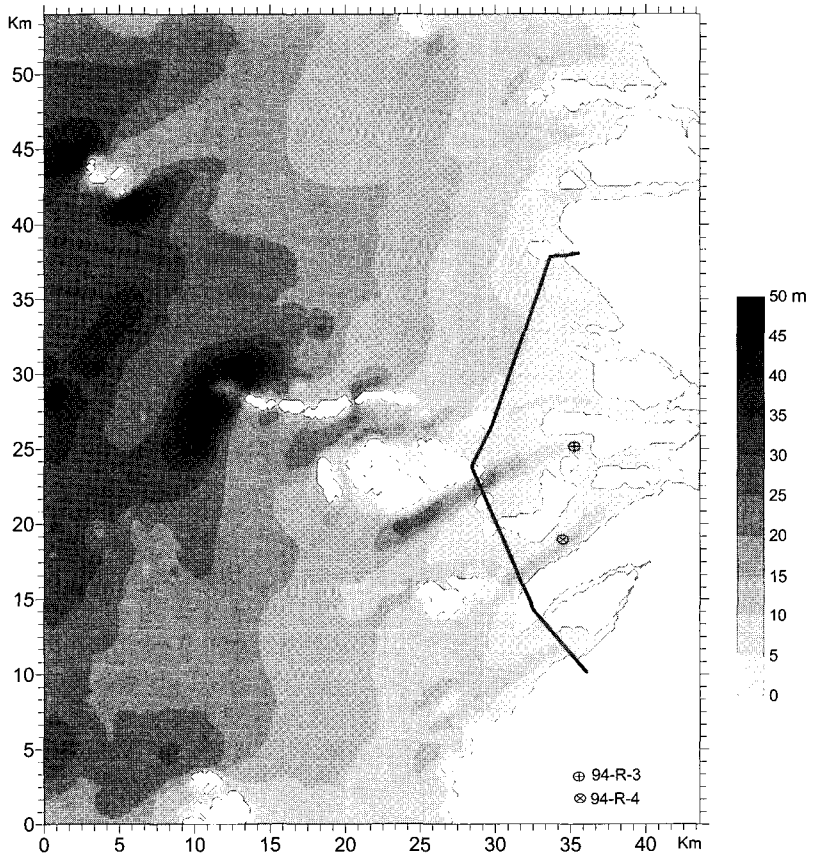

Fig. 1. The extent and depth map of the study area. The bold line indicates the sea dike system. Symbols ⊕ and ⊗ show the locations of tidal current measurement 94-R-3, 94-R-4.

The data on sea water temperature and salinity are taken from the field surveys carried out in the summer 1992 and winter 1993 by Marine Development Institute of Kunsan National University (Kim, 1994). The observed locations mainly concentrated surrounding both sides of the sea dike and inside of the reclamation area. In order to set the values of temperature and salinity for the whole numerical model area the interpolation and extrapolation are applied.

The wind data obtained from the observed data in the 1969-1977 time period of the Kunsan Meteorological Observatory and the discharges from Geum, Mankyung and Dongjin rivers obtained based on the experience formula(the Ministry of Construction, Korea, 1993) are shown in Table 1 and 2.

The model is calibrated by using the above mentioned harmonic constants and tidal currents measured at the stations 94-R-3 and 94-R-4. The calculated co-range and co-tidal charts of 4 tidal constituents are presented in Fig. 2. Generally, their patterns are similar with the correspondent charts produced by the National Oceanographic Research Institute, Ministry of Maritime Affairs and Fisheries. The calculated and observed harmonic constants of 4 tidal constituents at Wi Island station are presented in Table 3. The southern open boundary of the numerical model set near this station, therefore, this comparison is just as a reference.

The calculated and observed tidal ellipses at the measurement locations 94-R-3 and 94-R-4 are presented in Fig. 3. It shows that the calculated tidal currents agree acceptably with the observed ones. The difference of the major axis of the tidal ellipse at 94-R-3 from the observational data may be due to the topography approximation of the numerical there.

On the basis of the obtained results, it is said that the numerical model is calibrated acceptably and can be apply to evaluate changes of both tidal and residual currents in the interested area before and after the construction of the sea dike system.

Table 1. Averaged wind in 4 seasons (adopted from the Kunsan Meteorological Observatory)

Season / Wind	Spring	Summer	Autumn	Winter
Speed (m/s)	3.95	3.95	4.10	3.80
Direction	WNW	WSW	WNW	WNW

Table 2. Seasonal discharges from three rivers (adopted from the Ministry of Construction).

Season / River	Spring	Summer	Autumn	Winter
Geum	1871.0	3124.0	1056.0	1263.0
Mankyung	23.0	90.0	17.0	8.0
Donhjin	20.0	74.0	17.0	8.0

Table 3. Calculated and observed harmonic constants of four tidal constituents at Wi Island station, amplitude in cm, phase in degree (referenced to 126°E).

Tidal constituent	M_2		S_2		K_1		O_1	
	Amp.	Phase	Amp.	Phase	Amp.	Phase	Amp.	Phase
Observed	192.4	64.4	74.3	114.9	35.6	270.9	24.1	234.9
Calculated	191.9	65.3	73.8	114.9	35.8	271.1	24.4	234.6

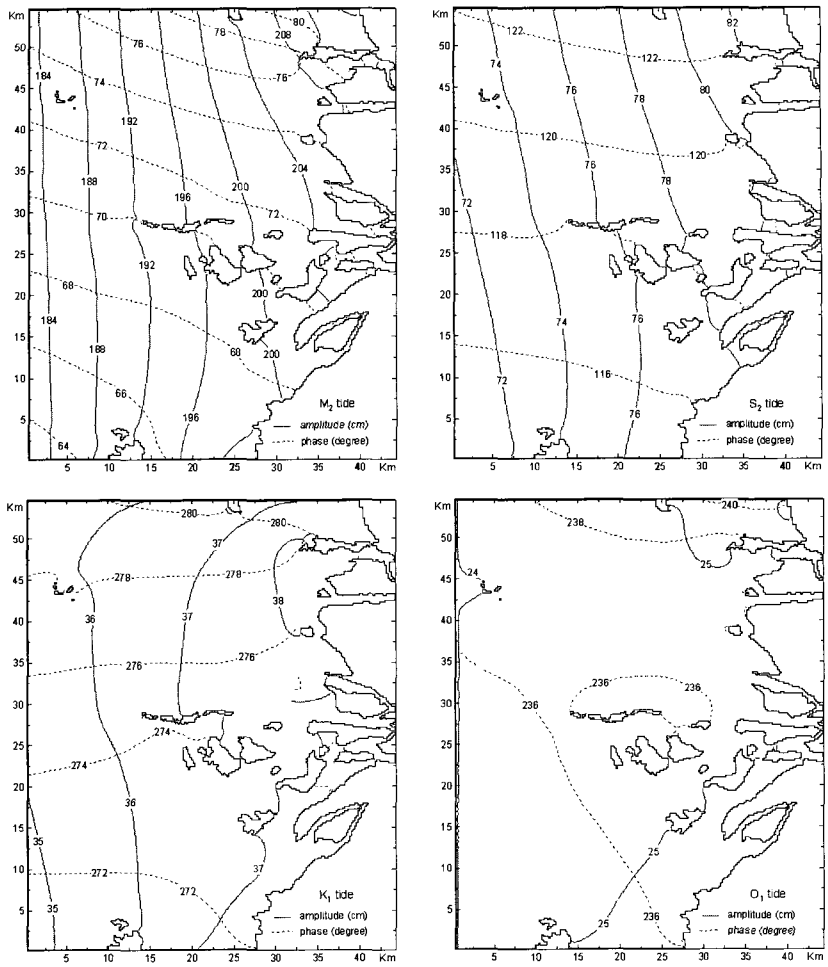

Fig. 2. Calculated co-range and co-tidal charts of 4 tidal constituents, M_2, S_2, K_1 and O_1, before construction of the sea dike system.

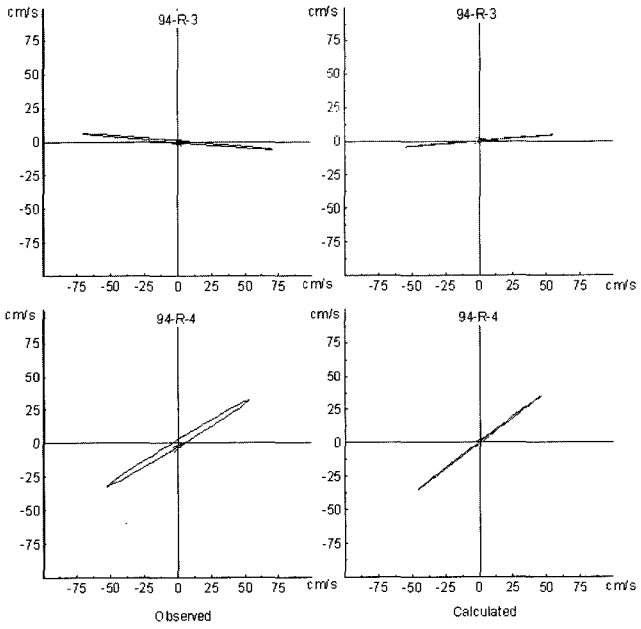

Fig. 3. Observed (left) and calculated tidal ellipses of M_2 tide at measured locations 94-R-3 and 94-R-4.

5. Changes of Tide and Tidal Current after the Sea Dike Construction

Using the same parameters of the numerical models (the depth map, grid sizes, open boundary conditions...), except the sea dike system is supposed to build completely, the propagations of M_2, S_2, K_1 and O_1 are calculated. The obtained results point out that the tidal levels and tidal currents are changed slightly out the sea dike. For example, the calculated amplitude of M_2 is changed about 2, 3 cm out the sea dike system, as shown in Fig. 4 and Fig. 5. It is shown that in the Case A-2, the tide amplitude out of the reclamation area is reduced and the propagation direction is changed to northwards. The changes of amplitudes and phases of S_2, K_1 and O_1 tides are small and not presented in this paper.

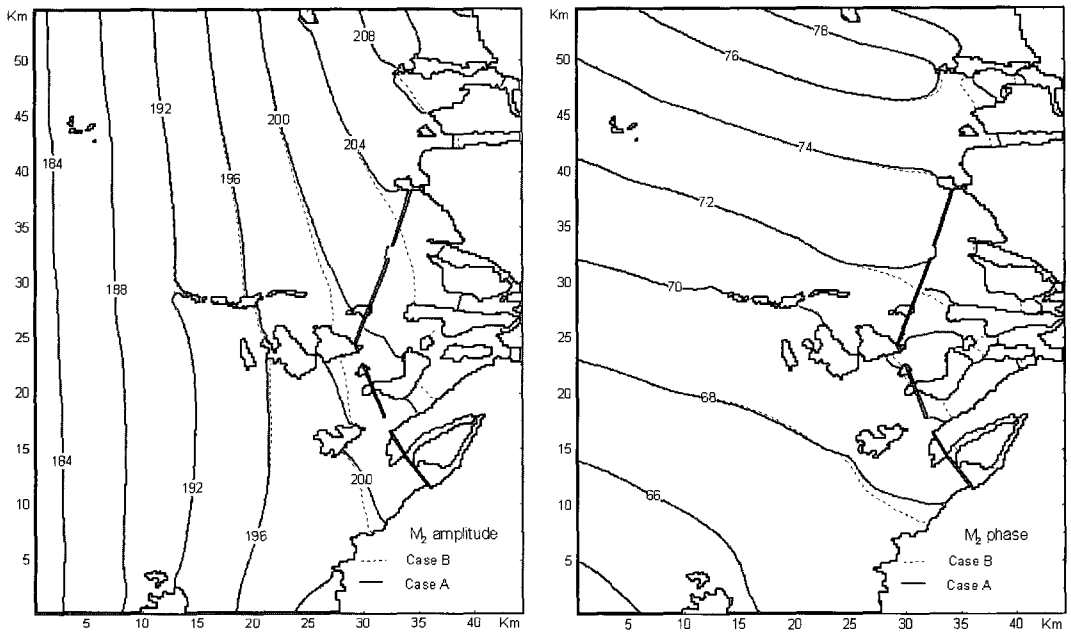

Fig. 4. Changes of amplitude (left) and phase (right) of M_2 tide in case a (the sea dike with 3 flow gates)

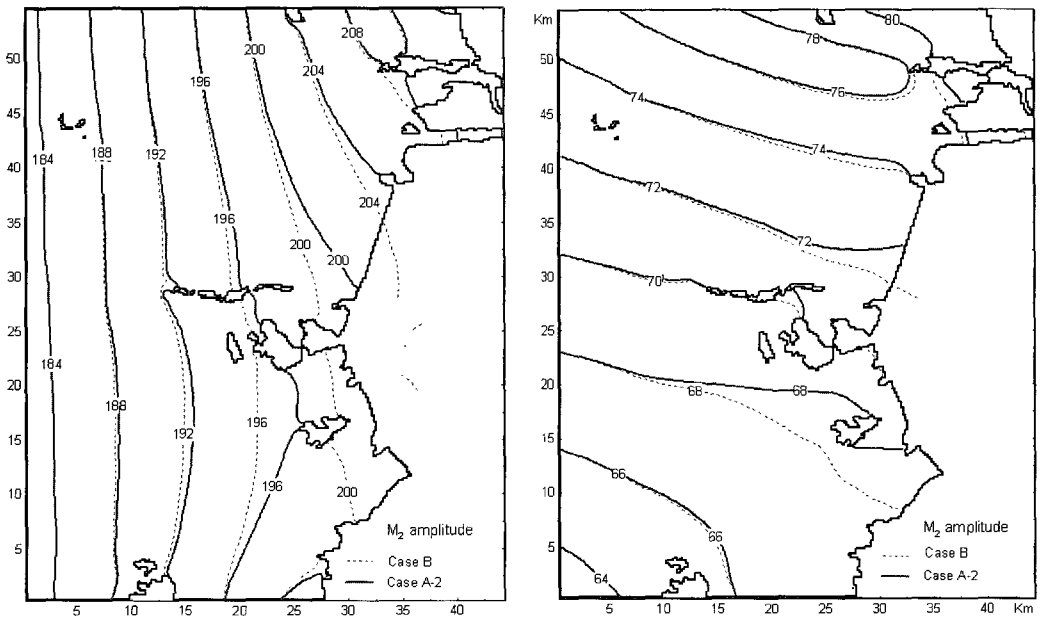

Fig. 5. Changes of amplitude (left) and phase (right) of M_2 tide in Case A-2, the sea dike without flow gates

The tidal current ellipses of M_2 tide before and after the sea dike construction (Case A) are presented in Fig. 6. It is clear that the tidal currents increase significantly near the flow gates where the M_2 current speeds can reach 1.9 m/s. The changes of M_2 current speed can be seen more clearly in Fig. 8 that shows subtracting the Case B from Case A. Similarly, the tidal current ellipses and speed changes of S_2 tide after the dike construction are shown in Fig. 7 and 8. In Fig. 9 the tidal ellipses and speed changes of M_2 in Case A-2 are presented. The amplitudes and speeds of K_1 and O_1 are quite small in comparison with the semi-diurnal tides and they are not presented here.

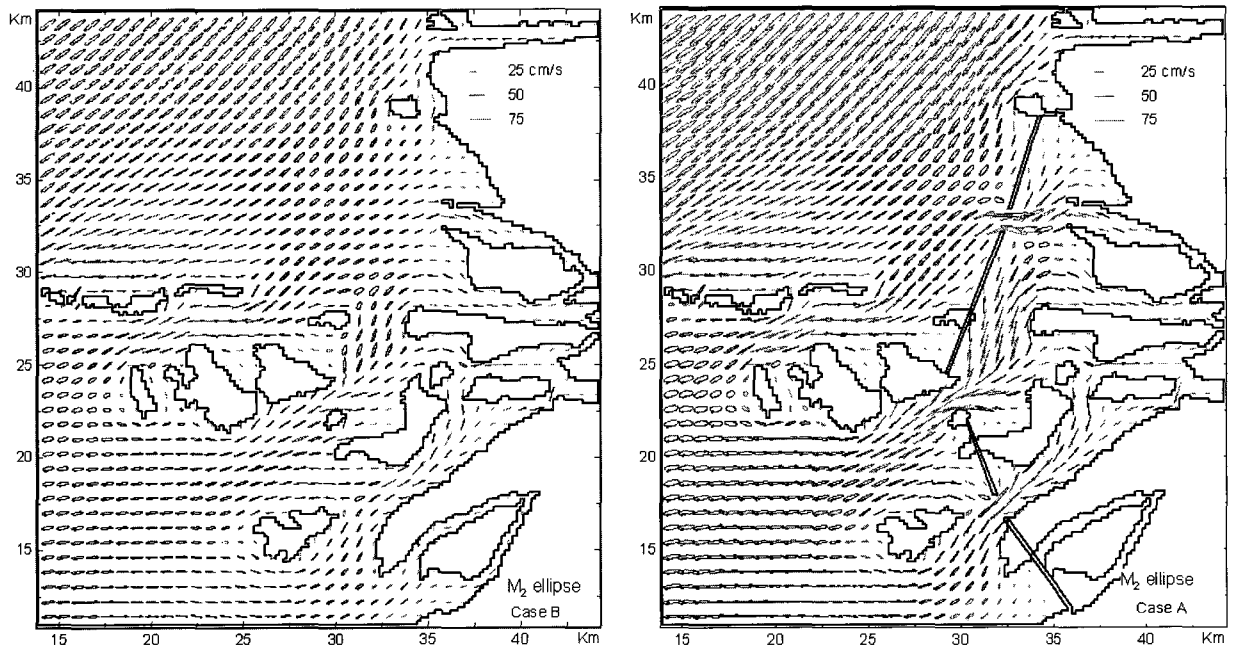

Fig. 6. Tidal current ellipses of M_2 tide in Case B (left) and Case A (right)

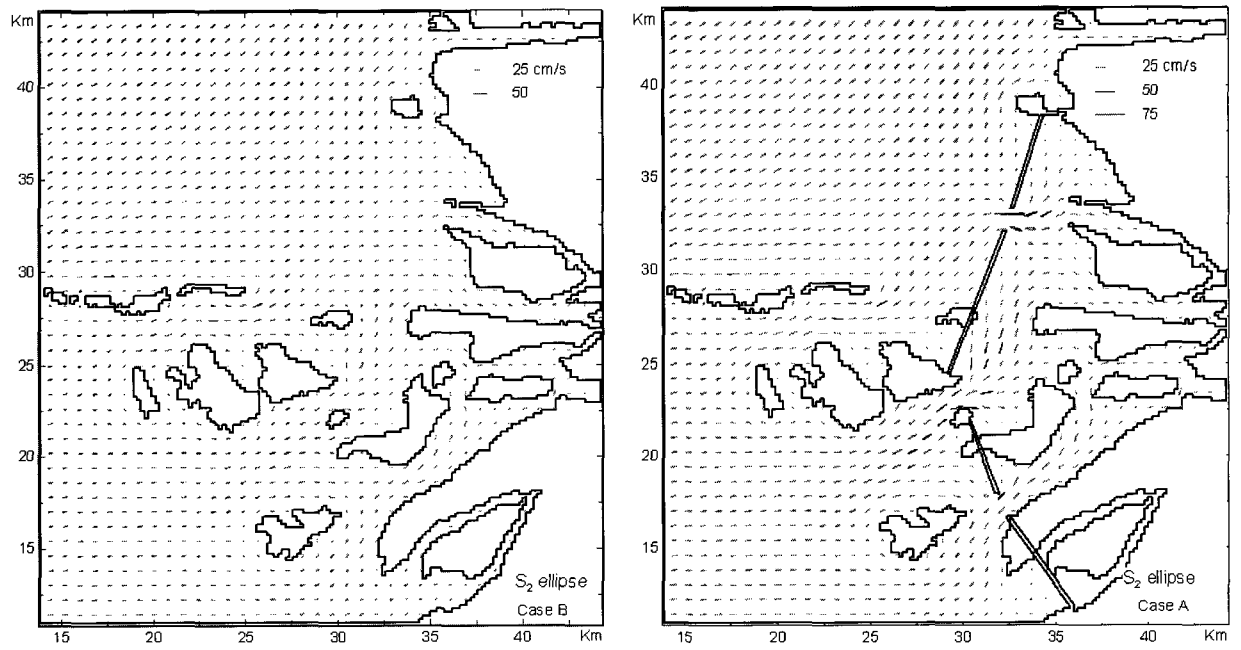

Fig. 7. Same as Fig. 6 but for S_2 tide

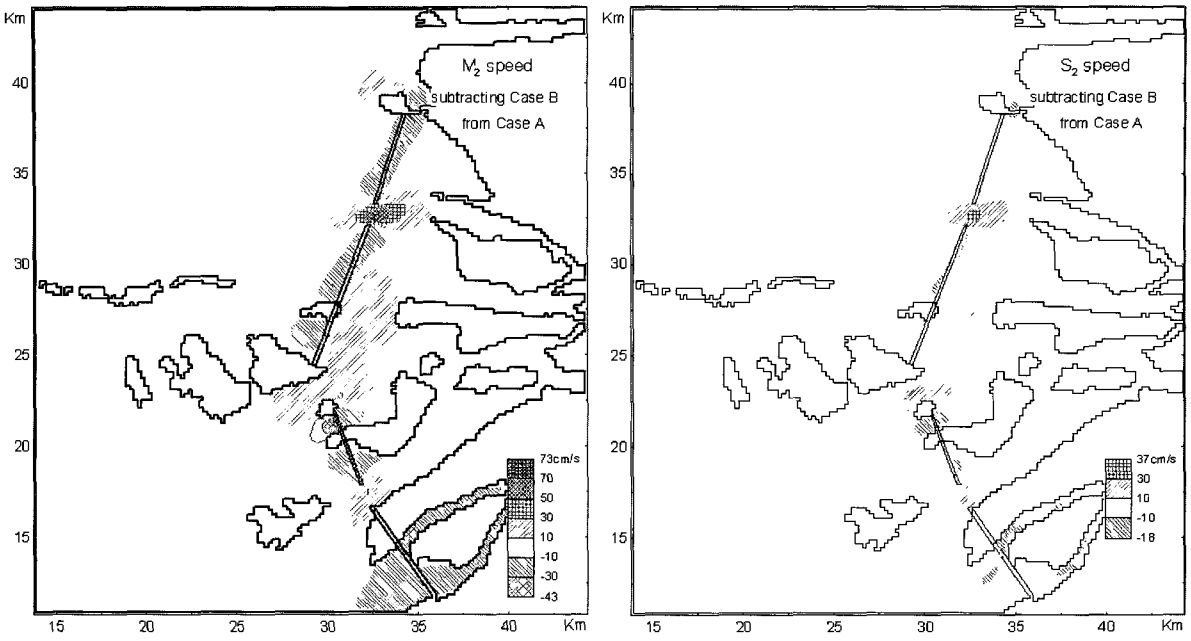

Fig. 8. Changes of M_2 (left) and S_2 (right) tidal current speeds in Case A in comparison with that of Case B

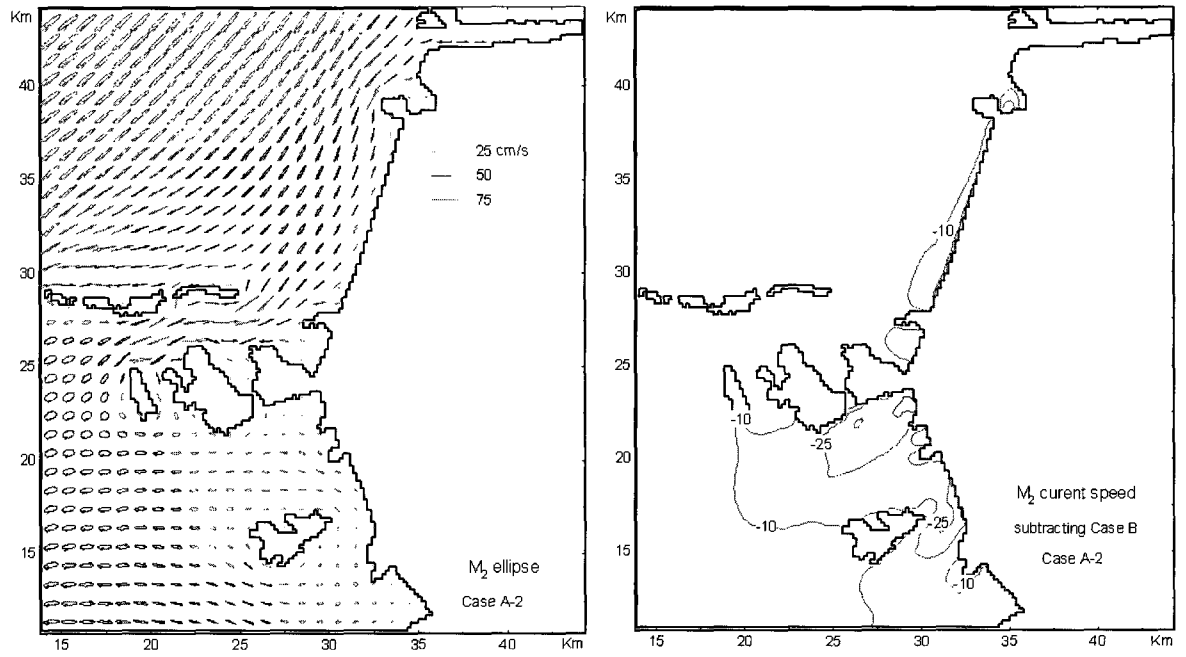

Fig. 9. Tidal ellipse of M_2 (left) and changes of it speeds (right) in Case A-2 in comparison with that of Case B

6. Changes of Residual Current after the Sea Dike Construction

As shown in the Table 1, the dominant wind directions in the Saemangeum area are WNW and WSW and the averaged wind speeds from season to season are not changed very much, about of 4m/s. The density-driven current does not play an important role in general circulation in this area, at least on the basis of our numerical experiments. Therefore, in order to investigate the characteristics of the residual flow in the study area the calculations for summer and winter are carried out.

The obtained results show that the tide-induced

residual flow plays the most important role in the study area and due to this happens throughout of years, therefore, the tide-induced flow is considered separately, first. The depth-averaged calculated tide-induced residual currents of M_2, S_2 and K_1 tides before and after the sea dike construction are presented in Figs. 10, 11 and 12. It is obvious that the M_2 tide induced residual flow is strongest. The speed can reach 10cm/s in the Case B and more than 20cm/s in the Case A.

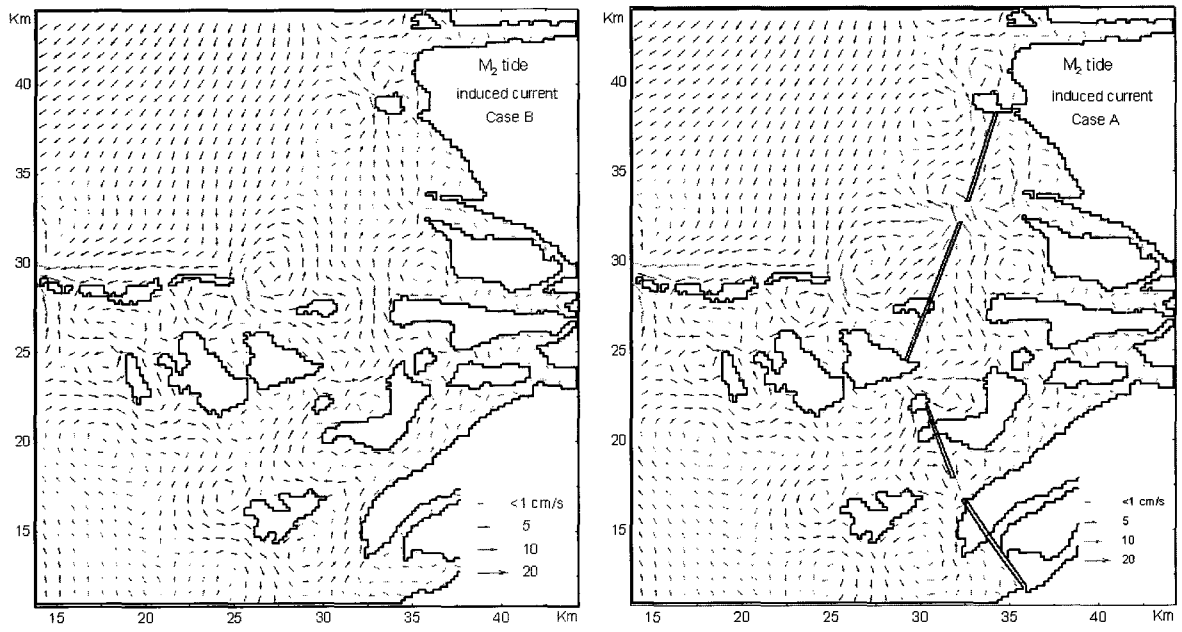

Fig. 10. Depth-averaged M_2 tide induced residual flow before (case B, left) and after (case A, right) sea dike construction

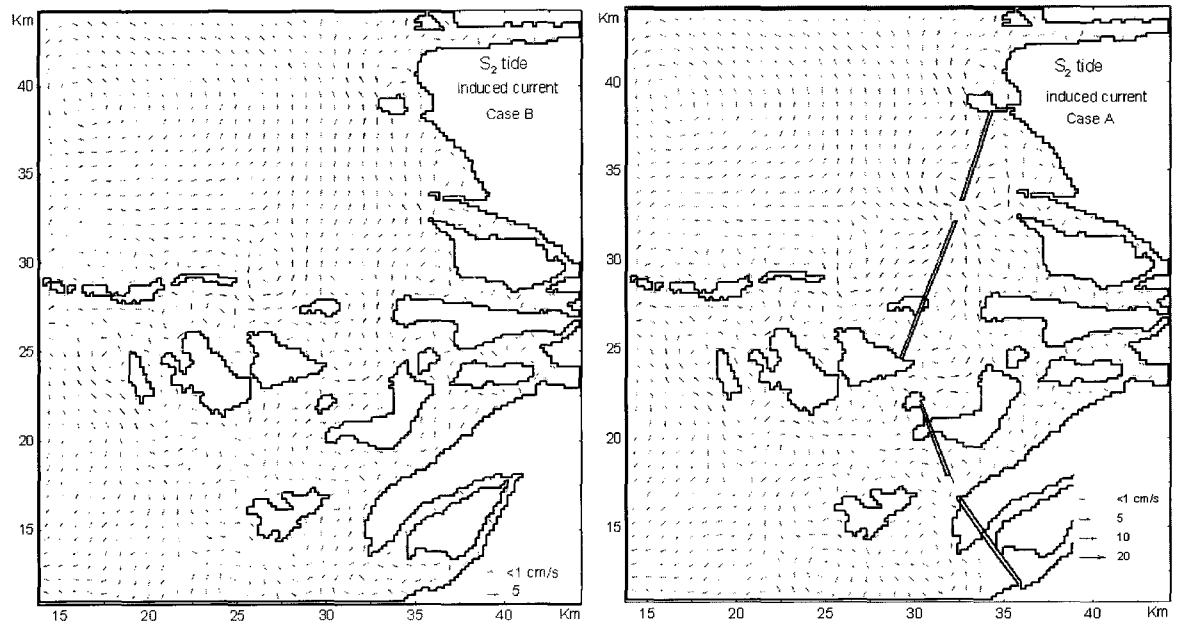

Fig. 11. Depth-averaged S_2 tide induced residual flow before (case B, left) and after (case A, right) sea dike construction

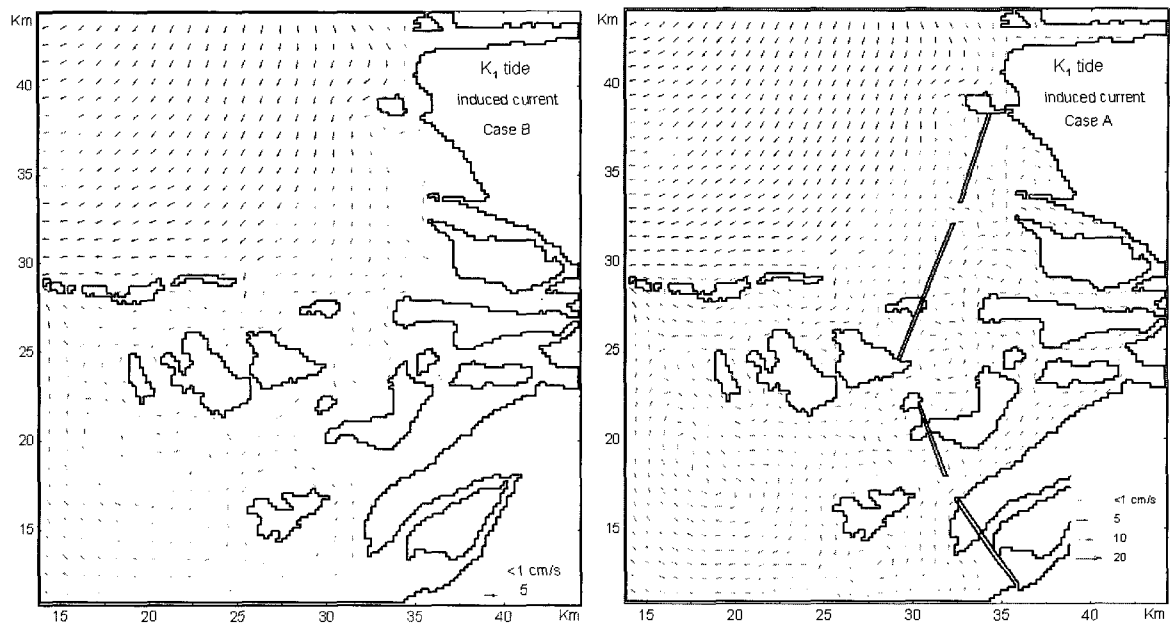

Fig. 12. Depth-averaged K_1 tide induced residual flow before (case B, left) and after (case A, right) sea dike construction

In the Case B, before the dike construction, the M_2 tide induced residual flow has a northward tendency in the reclamation area. In the Case A, the M_2 tide induced residual flow becomes rather strong and there are clockwise and counter clockwise eddies not only in the northern flow gate region but also in the southern part of the reclamation area, as shown in Fig. 10. The calculated results of the S_2 tide induced residual flow shows the nearly similar patterns of current in the reclamation area, but their speeds are much smaller, the maximum speed is about 10 cm/s. The K_1 and O_1 tide induced residual currents are quite small.

Finally, the residual flow, including tide-induced residual, wind-driven, density driven and river discharge components, in summer and winter are calculated. The calculated results at the upper (surface) and the lower (at depth of 15m) layers are presented in Fig. 13 and Fig. 14.

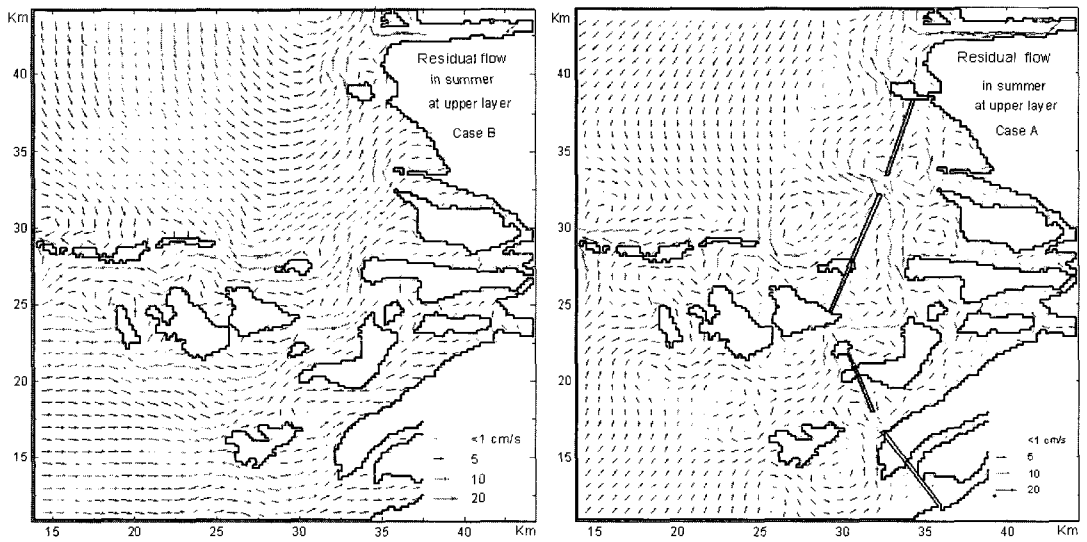

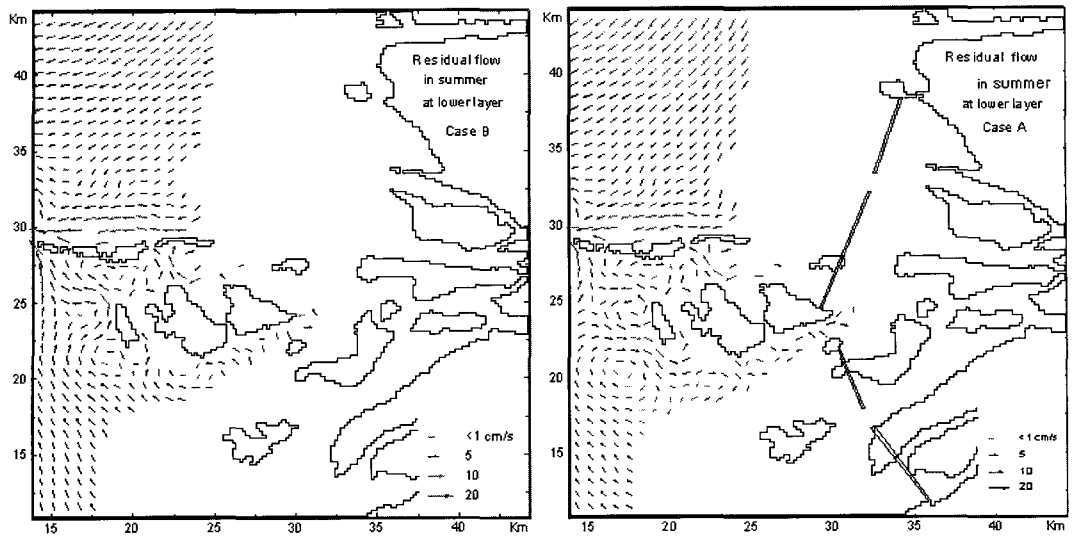

Fig. 13. Residual flow in summer at upper and lower layers, before (case B, left) and after (case A, right) sea dike construction

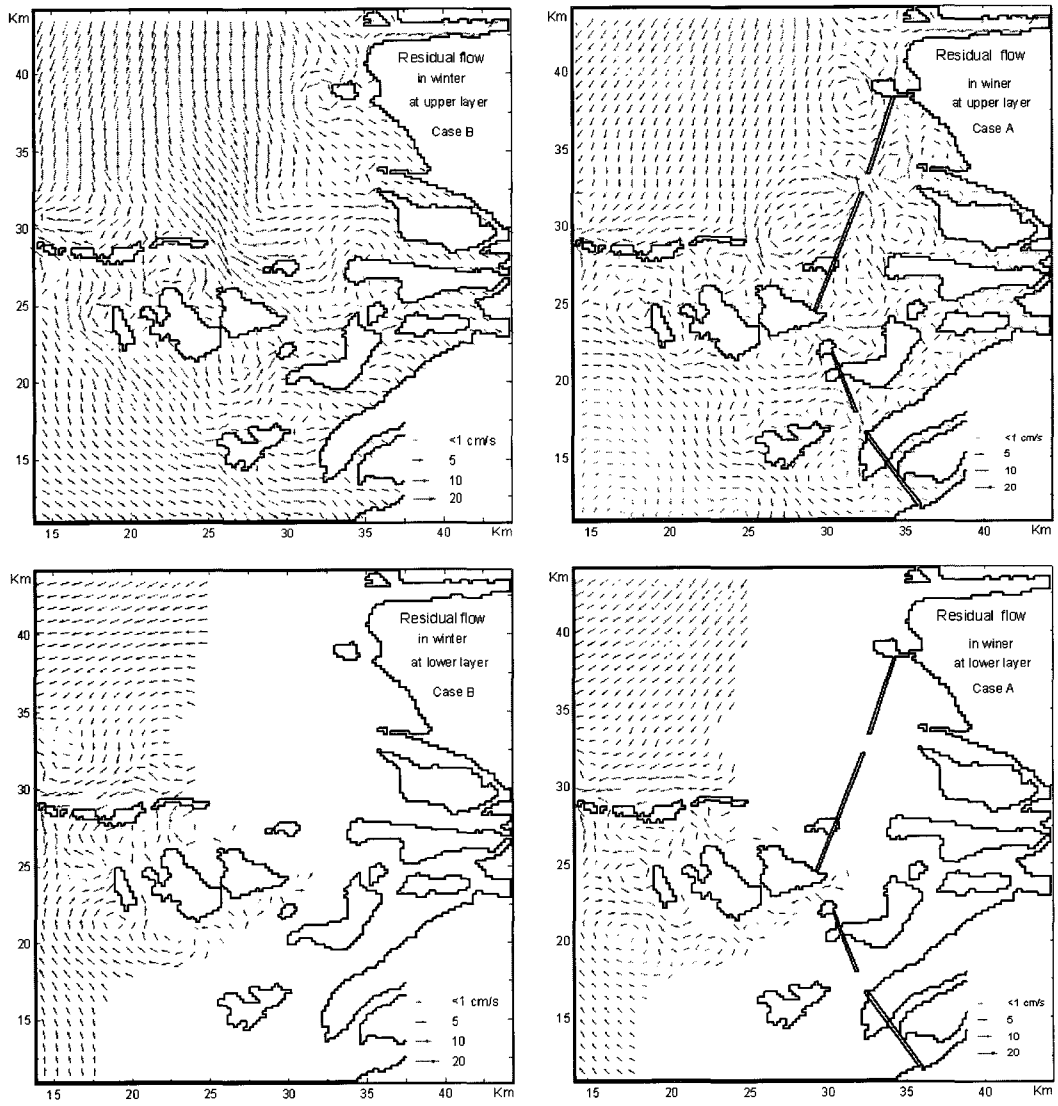

Fig. 14. Residual flow in winter at the upper and the lower layers, before(case B, left) and after (case A, right) sea dike construction

The calculated results of Case B, before the sea dike construction, show that in summer, at the upper layer , as shown in Fig. 13 (top-left panel), the residual current direction is eastward in the south-west part, then changes to northward in the reclamation area, and has a counter-clockwise circulation in northern part. At the lower layer, the current direction is north-westward part and south-westward in the north. There are several eddies between islands.

In winter, before the sea dike construction, at the upper layer the residual current, flow from north to south generally but from west to east in the reclamation area. At the lower layer the current patterns are almost the same as that in summer as shown in Fig. 15. It means at the upper layer the wind-driven component have a significant influence on the residual flow pattern, while at the lower layers the tide-induced component drives the current pattern.

The results of Case A, after sea dike construction, show that the residual currents are influenced mainly by tide-induced residual component in the reclamation area in both summer and winter. That results in the same flow pattern in summer and winter in this area. The residual currents in regions out of the reclamation area are not changed significantly in comparison with the Case B.

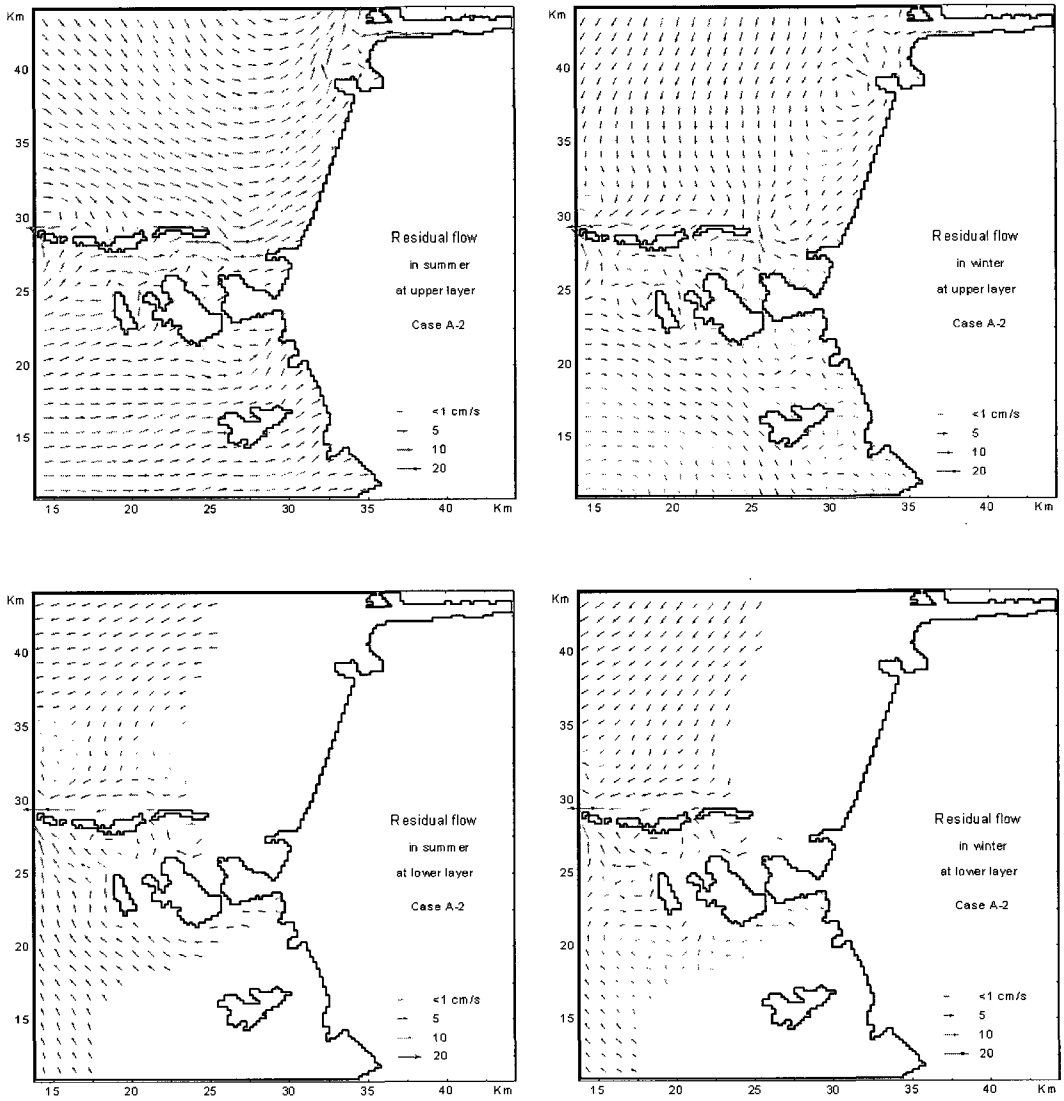

Fig. 15. Residual flow in summer (left) and winter (right) at three layers, upper, middle and lower in Case A-2

7. Conclusions

A hydrodynamics numerical model was used to investigate the effects of the dike construction on both tidal and residual currents in the Saemangeum tide land reclamation area. Our numerical solutions show that the co-range and co-tidal charts change slightly out the reclamation area after the sea dike construction. The tidal amplitude is reduced and tidal phase is delayed significantly in the reclamation. The tidal currents at the flow gates appear to be very strong enough M_2 and S_2 tidal current can reach 1.9 m/s and 0.8 m/s respectively. This strong tidal current results in a strong tide-induced residual flow. Around the flow gates, the residual flow is strong, about 30cm/s, and there exist several clockwise and counter clockwise eddies alternately. The wind-driven current gives a significant influence on the residual flow pattern at the upper layer off the reclamation area. In the reclamation area the residual currents in summer and in winter are almost same, because they are driven mainly by the tide-induced residual component. The influences of the outflows from Mankyung and Dongjin rivers appear to be minor.

References

1. Blumberg A.F., and Kantha, L.H. (1985). "Open boundary condition for circulation models." *Journal of Hydraulic Engineering*, ASCE, Vol. 111, No. 2, pp. 237-255.
2. Blumberg A.F., and Mellor, G.L. (1987). "A Description of three dimensional coastal ocean circulation model." *Three-Dimensional Coastal Model Ocean Models*, American Geophysical Union, Washington D.C., pp. 1-16.
3. Choi, B. (1990). "Preliminary estimation of barrier effects on tides in Saemanguem area." *Journal of KSCOE*, Vol. 2, No. 1, pp. 34-42.
4. Kim, G.R (1994). *Fishery damage compensation report of Saemangeum development work*, Coastal Research Center, Kunsan National University.
5. Kim, D.-G. , Seo, I.W., Back, K.O., and Sonu, J.H. (1997). " Prediction of influence of polluted water discharged from Saemankeum lake." *J. of KWRA*, Vol.30, No. 6, pp. 649-659.
6. Lee, S.H., Choi, H.Y., Son, Y.T., Kwon, H.K., and Kim. Y.-K. (2003). "Low-salinity water and circulation in summer around Saemangeum area in the west coast of Korea." *The Sea, J. of KSO*, Vol. 8. No. 2, pp. 138-150.
7. Manh D.V., and Yanagi, T. (1997). "A three-dimensional numerical model of tides and tidal currents in the Gulf of Tongking." *La mer*, Vol. 35, pp. 15-22.
8. Manh D.V., and Yanagi, T. (1999). "A study on residual flow in the Gulf of Tongking." *Journal of Oceanography*, Vol. 56, pp. 59-68.
9. Nihoul J.C.J., and Jamart, B.M. (1987). *Three-dimensional models of marine and estuarine dynamics*, Elsevier Science Publishers B. V., pp. 35-54.
10. Park, Y.K. (2000). "Estimation on parameters of water quality in the Saemanguem lake by WASP5 model." *J. of KSEE*, Vol. 22, No. 4, pp. 743-754.
11. Rural Research Corporation of Korea (1988). *Pre-estimate of seawater surface and change of accumulation layer on sub-aqueous in Saemangeum coastal area*, pp. 373-392.
12. Rural Research Corporation of Korea (1994). *Survey of wave and hydraulic experiment in Saemangeum coastal area*, pp. 331-340.
13. Shin, M.S., Lee, J.N., and Hong, S.K. (1994). "Development of Model by Soil Diffusion within Dam." *Hydro-Port94*, October 19-21, Yokosuka, Japan.
14. Vreugdenhil C.B. (1994). *Numerical method for shallow water flow*, Kluwer Academic Publishers, pp. 217-247.
15. Yanagi, T., Okada, S., and Tsukamoto, K.(1992). "Numerical simulation of dispersal patterns of red sea bream juveniles, Pagrus major, in Nyuzu Bay, Japan." *Journal of Marine System*, Vol. 3, pp. 477-487.

(논문번호:04-105/접수:2004.11.20/심사완료:2004.12.30)

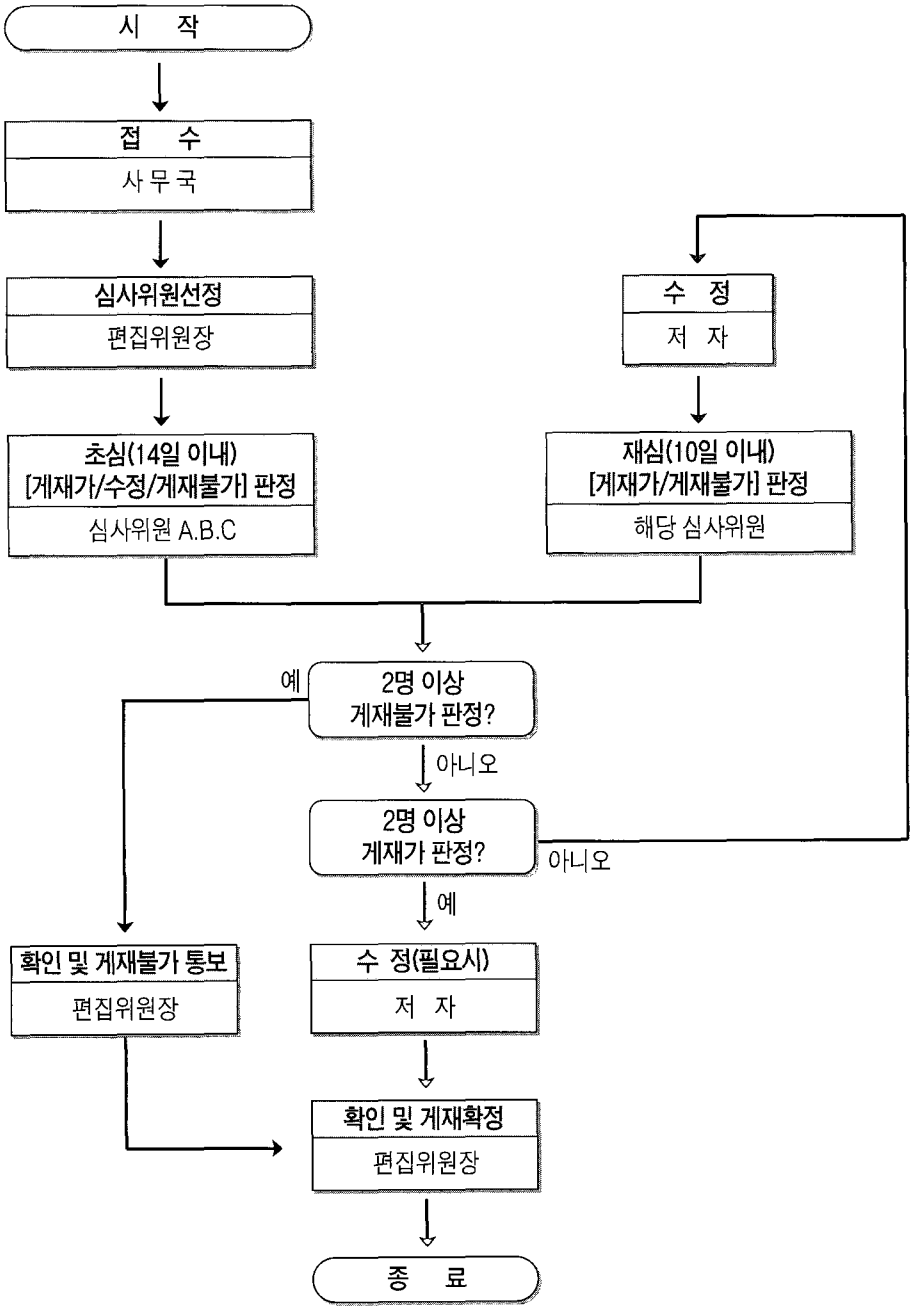

한국수자원학회 논문심사 흐름도

* 논문심사에 소요되는 기간은 초심(14일 이내)과 재심(10일 이내)을 포함하여 3개월 이내에 처리함을 원칙으로 하며, 논문심사와 관련된 행정처리는 학회 사무국이 담당한다. 저자가 6개월 이내에 논문수정에 응하지 않을 경우 게재불가로 처리한다. 토의 및 회답은 논문집 편집위원회에서 처리한다.